Earth and Planetary Science Letters 353–354 (2012) 198–207

Contents lists available at SciVerse ScienceDirect

Earth and Planetary Science Letters

journal homepage: www.elsevier.com/locate/epsl

The distribution of neodymium isotopes and concentrations in the Eastern Equatorial Pacific: Water mass advection versus particle exchange

Patricia Grasse [a,*], Torben Stichel [a,b], Roland Stumpf [a], Lothar Stramma [a], Martin Frank [a]

[a] Helmholtz Centre for Ocean Research Kiel (GEOMAR), Wischhofstraße 1-3, 24148 Kiel, Germany
[b] University of Hawaii-Manoa, 1680 East-West Road, Honolulu, HI 96822, United States

ARTICLE INFO

Article history:
Accepted 30 July 2012
Editor: P. DeMenocal

Keywords:
neodymium isotopes
Rare Earth Elements
particle scavenging
boundary exchange
oxygen minimum zone
Eastern Equatorial Pacific

ABSTRACT

The radiogenic isotope composition of the Rare Earth Element (REE) neodymium (Nd) is a powerful water mass proxy for present and past ocean circulation. The processes controlling the Nd budget of the global ocean are not quantitatively understood and in particular source and sink mechanisms are still under debate.

In this study we present the first full water column data set of dissolved Nd isotope compositions and Nd concentrations for the Eastern Equatorial Pacific (EEP), where one of the globally largest Oxygen Minimum Zones (OMZ) is located. This region is of particular interest for understanding the biogeochemical cycling of REEs because anoxic conditions may lead to release of REEs from the shelf, whereas high particle densities and fluxes potentially remove the REEs from the water column. Data were obtained between 1°40′N and 16°S along a nearshore and an offshore transect. Near surface zonal current bands, such as the Equatorial Undercurrent (EUC) and the Subsurface Countercurrent (SSCC), which are supplying oxygen-rich water to the OMZ are characterized by radiogenic Nd isotope signatures ($\varepsilon_{Nd}=-2$). Surface waters in the northernmost part of the study area are even more radiogenic ($\varepsilon_{Nd}=+3$), most likely due to release of Nd from volcanogenic material. Deep and bottom waters at the southernmost offshore station (14°S) are clearly controlled by advection of water masses with less radiogenic signatures ($\varepsilon_{Nd}=-7$) originating from the Southern Ocean. Towards the equator, however, the deep waters show a clear trend towards more radiogenic values of up to $\varepsilon_{Nd}=-2$. The northernmost station located in the Panama basin shows highly radiogenic Nd isotope signatures in the entire water column, which indicates that particle scavenging, downward transport and release processes play an important role. This is supported by relatively low Nd concentrations in deep waters (3000–6000 m) in the EEP (20 pmol/kg) compared to locations in the Northern and Central Pacific (40–60 pmol/kg), which suggests enhanced removal of Nd in the EEP.

1. Introduction

The radiogenic isotope composition of the Rare Earth Element (REE) neodymium (Nd) is a powerful water mass tracer for the present and past ocean due to its intermediate oceanic residence time (360–1900 yr) and the fact that it is independent of biological fractionation processes (Piepgras et al., 1979; Jeandel et al., 1995; Frank, 2002; Tachikawa et al., 2003; Arsouze et al., 2007, 2009).

The Nd isotope composition ($^{143}Nd/^{144}Nd$) is expressed as ε_{Nd}. ε_{Nd} corresponds to the deviation of the measured $^{143}Nd/^{144}Nd$ of the samples from CHUR (Chondritic Uniform Reservoir with $^{143}Nd/^{144}Nd=0.512638$, Jacobsen and Wasserburg, 1980) in parts per 10,000: $\varepsilon_{Nd}=[(^{143}Nd/^{144}Nd_{sample}/^{143}Nd/^{144}Nd_{CHUR})-1]\times 10.000$. The Nd isotope composition of water masses is primarily controlled by the isotopic composition of the surrounding landmasses at their origin. Weathering of young mantle-derived rocks surrounding the Pacific Ocean leads to more radiogenic values compared to the Atlantic Ocean with its margin predominantly composed of old continental crust. In addition water masses from the northern Pacific and from the Southern Ocean are clearly labeled by distinct isotopic fingerprints. North Pacific water masses, such as North Pacific Deep Water (NPDW) and North Pacific Intermediate Water (NPIW) show more radiogenic values ($\varepsilon_{Nd}=-3$ to $\varepsilon_{Nd}=-5$, Piepgras and Jacobsen, 1988; Amakawa et al., 2004, 2009) compared to water masses originating from the Southern Ocean ($\varepsilon_{Nd}=-8$ to $\varepsilon_{Nd}=-9$, Piepgras and Wasserburg, 1982; Stichel et al., 2012). The exact input mechanisms and the influence of weathering processes on the Nd isotope composition and Nd concentration of seawater are not yet

* Correspondence to: Helmholtz Centre for Ocean Research Kiel (GEOMAR), Wischhofstrasse 1-3, 24148 Kiel, Germany. Tel.: +49 431 600 2507; fax: +49 431 600 2925.
E-mail address: pgrasse@geomar.de (P. Grasse).

0012-821X/$ - see front matter © 2012 Elsevier B.V. All rights reserved.
http://dx.doi.org/10.1016/j.epsl.2012.07.044

fully understood but it has become clear that besides eolian and riverine inputs (Goldstein et al., 1984; Goldstein and Jacobsen, 1988; Elderfield et al., 1989; Henry et al., 1994; Sholkovitz et al., 1999) also processes at the continent–seawater interface, so called "boundary exchange processes" must play an important role or may even dominate the inputs (Lacan and Jeandel, 2005; Arsouze et al., 2007, 2009). In contrast, the contribution of Nd to the ocean via hydrothermal inputs has been suggested to be negligible. In fact, hydrothermal vents rather have to be considered a sink of REEs in the global ocean budget together with particle scavenging processes (German et al., 1990; Klinkhammer et al., 1983; Halliday et al., 1992). The importance of particle scavenging and release processes is most notably documented by the nutrient-like vertical distribution of the concentrations of most REEs (e.g. Elderfield and Greaves, 1982). At the same time numerous studies have demonstrated that Nd isotopes clearly label particular water masses that can be followed across entire ocean basins. This phenomenon has been named the "Nd paradox" (Jeandel et al., 1995; Tachikawa et al., 1999; Siddall et al., 2008). To better understand the processes influencing the isotope composition as well as the concentration gradients in the ocean, several modeling studies were conducted (Tachikawa et al., 2003; Arsouze et al., 2007, 2009; Jones et al., 2008; Siddall et al., 2008; Oka et al., 2009). Although inclusion of boundary exchange processes has improved the modeled isotope and concentration distributions it still seems that there are additional sources and sinks of Nd. To resolve these uncertainties a comprehensive data set for the global distribution of Nd isotope compositions, as well as Nd concentrations is required for the global ocean, a goal that is currently being pursued by the international GEOTRACES program. Since 1980 a large number of dissolved Nd isotope data from the Atlantic Ocean have been published but data from the Pacific Ocean are scarce (Piepgras et al., 1979; Piepgras and Wasserburg, 1982; Piepgras and Jacobsen, 1988; Amakawa et al., 2000, 2004, 2009; Vance et al., 2004; Lacan and Jeandel, 2001; Shimizu et al., 1994).

In this study we present the first comprehensive data set of dissolved Nd isotope and Nd concentration data for the Eastern Equatorial Pacific (EEP). The aim is to investigate their behavior, as well as the reliable use of Nd isotopes as water mass tracer, under the influence of a coastal high productivity environment characterized by high particle densities and exchange processes of the coastal waters with the shelf sediments.

1.1. Currents and water masses of the Eastern Tropical Pacific

The general oceanography of EEP is governed by intense upwelling and northward flowing surface currents, such as the Peru Oceanic Current (POC), the Peru Coastal Current (PCoastalC) and the Peru Chile Current (PCC), which can be found approximately 100–300 km offshore (Fig. 1a). These water masses originate in subantarctic regions (Strub et al., 1998; Penven et al., 2005; Karstensen and Ulloa, 2008). The Subantarctic Water (SAAW) which is transported to the EEP also from the south is a low salinity surface water mass which is subducted towards the equator to a depth around 100–200 m (Silva et al., 2009). Persistent easterly trade and alongshore winds produce offshore Ekman transport of surface waters, which causes the upwelling of nutrient-rich subsurface water to the euphotic zone (Brink et al., 1983). In equatorial regions westward flowing surface currents, such as the South Equatorial Current (SEC) produce an eastward pressure gradient. This force drives the Equatorial Undercurrent (EUC) and the Southern Subsurface Countercurrent (SSCC) to flow eastward along the equator and supply oxygen-rich waters to the upwelling area (Brink et al., 1983; Toggweiler et al., 1991; Fiedler and Talley, 2006). During austral summer 2009, when the samples for this study were taken, the EUC encountered the western coast of South America at approximately 0°N to 1°N at a core depth of 90 m (Czeschel et al., 2011). Together with the primary Southern Subsurface Countercurrent (pSSCC) and the

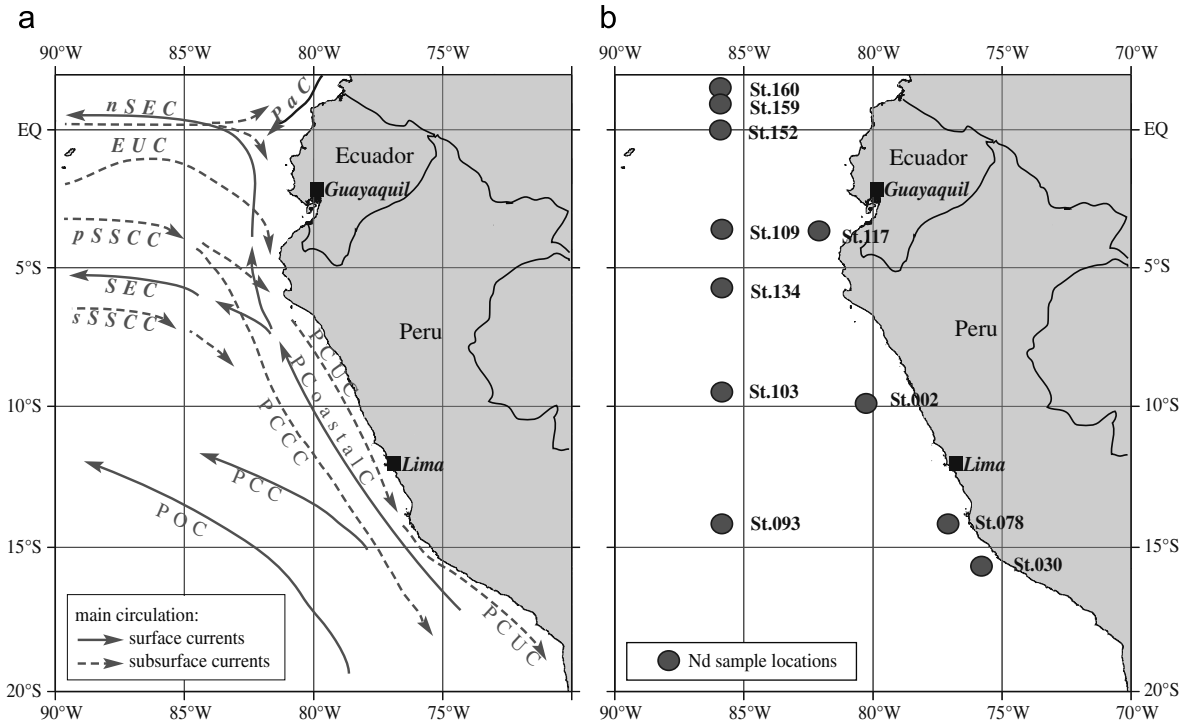

Fig. 1. (a) Schematic surface (solid gray lines) and subsurface (dashed gray lines) currents off Peru; and (b) sampling locations for Nd isotopes and concentrations during R/V Meteor cruises M77-3 and M77-4 (PaC: Panama Current, EUC: Equatorial Undercurrent, pSSCC: primary Southern Subsurface Contercurrent, sSSCC: secondary Southern Subsurface Countercurrent, SEC: South Equatorial Current, PCUC: Peru Chile Undercurrent, PCC: Peru Chile Current, PCCC: Peru Chile Countercurrent, POC: Peru Oceanic Current) (after Strub et al., 1998; Penven et al., 2005; Kessler, 2006; Ayon et al., 2008; Karstensen and Ulloa, 2008; and ADCP data according to Czeschel et al., 2011).

secondary Southern Subsurface Countercurrent (sSSCC) these currents are feeding the Peru Chile Undercurrent (PCUC) and account for up to 30% of its volume (Montes et al., 2010). The PCUC is the source water mass of the coastal upwelling and flows southward along the shelf at approximately 50–150 m water depth (Huyer et al., 1987; Penven et al., 2005; Karstensen and Ulloa, 2008).

The intermediate waters between 200 m and 1500 m water depth show a complex water mass structure. Eastern Pacific intermediate waters mainly consist of 3 water masses (Bostock et al., 2010 and references therein): North Pacific Intermediate Water (NPIW), Antarctic Intermediate Water (AAIW) and the Equatorial Pacific Intermediate water (EqPIW, see also Fig. 2). AAIW is primarily formed in the southeast Pacific, just off the coast of southern Chile where it is subducted and flows northward to a latitude of approximately 20°S (Talley, 1999; Kawabe and Fujio, 2010). NPIW is formed in the northwestern subtropical gyre along the Kuroshio and Oyashio Front (Talley, 1993) and is generally characterized by lower oxygen concentrations (<150 μmol/kg) than its Southern Hemisphere counterpart, the AAIW (200–300 μmol/kg, Table 1; Bostock et al., 2010).

Unlike the Atlantic Ocean, the Pacific Ocean has no high-latitude northern source of deep water. The densest water mass in the Pacific basin is the Lower Circumpolar Deep Water (LCDW; Wijffels et al., 1996). The LCDW transforms into North Pacific Deep Water (NPDW), which is again modified by admixture of Upper Circumpolar Deep Water (UCDW) near the Hawaiian Islands. From there NPDW broadly flows southward along the continental slope of Central and South America and contributes to the mixture of deep water masses off Peru (Wijffels et al., 1996; Kawabe and Fujio, 2010). For the distinction of deep water masses temperature–salinity characteristics are ambiguous because NPDW and LCDW are very similar both in salinity and temperature. But NPDW can be easily distinguished by significantly higher silicate concentrations and lower oxygen concentrations than LCDW.

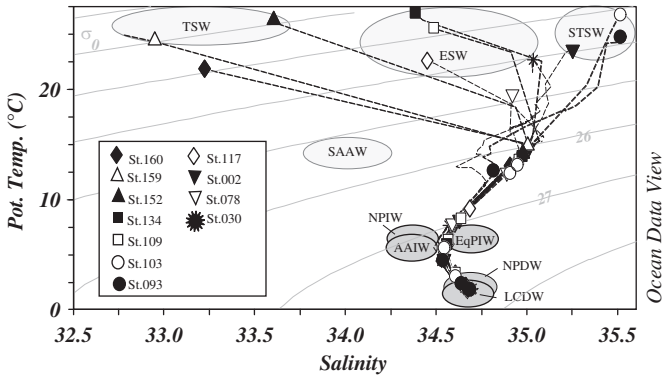

Fig. 2. *T–S* diagram with potential density (σ_θ) for the 11 stations of this study. Offshore stations are listed in the left column and nearshore stations in the right column of the inset legend. TSW: Tropical Surface Water, ESW: Equatorial Surface Water, STSW: Subtropical Surface Water, SAAW: Subantarctic Water, EqPIW: Equatorial Intermediate Water, NPIW: North Pacific Intermediate Water, AAIW: Antarctic Intermediate Water, NPDW: North Pacific Deep Water, LCDW: Lower Circumpolar Deep Water are marked according to Wijffels et al. (1996), Johnson and Toole (1993), Fiedler and Talley (2006) and Silva et al. (2009), see also Table 1.

2. Methods

The Samples were collected in the EEP between December 2008 and February 2009 aboard the German research vessel Meteor (M77/3 and M77/4) as part of the German-led Collaborative Research Centre "SFB 754" (Climate - Biogeochemistry Interactions in the Tropical Ocean, www.sfb754.de). The samples were taken at 7 stations along a longitudinal offshore section at 85°50′W between 1°40′N and 14°S and at 4 nearshore stations at distances between 100 km and 200 km from the coast between 3°35′S and 16°S (Fig. 1b). Seawater samples for analyses of Nd concentrations and isotope compositions were collected using a Seabird CTD Rosette System equipped with an O_2-sensor. Nutrient concentrations were measured following Grasshoff et al. (1999). Oxygen concentrations were determined with the O_2-sensor of the CTD and were later calibrated with bottle data obtained by Winkler titration (Winkler, 1888).

For Nd isotope analysis 20 L of seawater were collected in previously acid cleaned LDPE cubitainers. The samples were filtered through 0.45 μm nitrocellulose acetate filters (Millipore®) within 2 h after sampling. From each filtered sample an aliquot of 2 L was separated for Nd concentration measurements. All samples were acidified to pH 2 with concentrated subboiled hydrochloric acid (0.5 ml/L). On board 500 μl Iron(III)Chloride solution (~1 g $Fe(III)Cl_3$/ml in 3 M HCl) was added to each 20 L sample and after 1 d of equilibration the samples were adjusted to pH 8 with ammonium hydroxide (25%, suprapure grade) to co-precipitate the dissolved REEs with the iron hydroxide. At GEOMAR (Kiel, Germany) REE separation from major element cations was performed using a cation exchange resin (Biorad® AG50W-X12 resin, 200–400 mesh-size, 0.8 mL resin bed). The Nd was further purified in a second column chemistry step (Eichrom® Ln Spec, 50–100 mesh-size, 2 mL resin bed). The applied column chemistry followed the methods of Barrat et al. (1996) and Le Fèvre and Pin (2005).

Nd isotope measurements were carried out on a *Nu plasma* MC-ICPMS as well as on a *Thermo Scientific* TIMS TRITON. Measured $^{143}Nd/^{144}Nd$ ratios were corrected for mass fractionation to $^{146}Nd/^{144}Nd=0.7219$. All measured $^{143}Nd/^{144}Nd$ ratios of this study were normalized to the accepted value of the JNdi-1 standard of 0.512115 (Tanaka et al., 2000).

Table 1
Abbreviations and hydrographic characteristics of water masses in the study area.

	Water mass	Pot. temp. (°C)	Salinity (PSU)	Pot. density (kg/m³)	$Si(OH)_4$ (μmol/kg)	Oxygen (μmol/kg)	References
AAIW	Antarctic Intermediate Water	3–5	34.3–34.5	27.1	5–80	200–300	Bostock et al. (2010)
EqPIW	Equatorial Pacific Intermediate Water	–	34.5–34.6	27.3	20–115	0–125	Bostock et al. (2010)
ESW	Equatorial Surface Water	<25	>34	–	–	–	Fiedler and Talley (2006)
LCDW	Lower Circumpolar Deep Water	0.85	34.7	–	~130	~200	Johnson and Toole (1993)
NPDW	North Pacific Deep Water	1.0–1.8	34.6–34.7	27.6–27.8	–	–	Amakawa et al. (2009)
NPIW	North Pacific Intermediate Water	6.4	33.9–34.1	26.8	50–130	0–150	Bostock et al. (2010)
SAAW	Subantarctic Water	11.5	33.8	25.7	5	4–6	Silva et al. (2009)
STSW	Subtropical Surface Water	–	>35	–	–	–	Fiedler and Talley (2006)
TSW	Tropical Surface Water	25	<34	–	–	–	Fiedler and Talley (2006)

Samples containing less than 10 ng of Nd were measured on the MC-ICPMS using a manual time resolved mode. External reproducibility (2σ) of the Nd isotope measurements ranged between 0.1 ε_{Nd} and 0.8 ε_{Nd} depending on the applied method and sample concentrations (Table 2). Duplicate measurements of samples and standards on the MC-ICPMS and on the TIMS resulted in identical isotope compositions within the external 2σ reproducibilities.

For Nd concentration measurements, 500 mL of filtered and acidified seawater were used. The concentrations were determined using an isotope dilution (ID) method (Heumann (1992) and references therein). A defined amount of $^{150}Nd/^{144}Nd$ spike was added according to the assumed concentrations and was left for equilibration for 1 wk. REEs were then separated from matrix elements following the same method as for the isotope measurements but only using one cation exchange column (Biorad® AG50W-X12 resin, 200–400 mesh-size, 0.8 mL resin bed). The external reproducibility of the Nd concentration measurements was approximately 2% (1σ). Blank values for isotope and concentration measurements ranged between 1% and 3% of the sample concentration and were considered as negligible.

3. Results

3.1. Vertical distribution of Nd isotope composition and concentration

In Fig. 3 the profiles of dissolved Nd concentrations and Nd isotope compositions for the offshore and nearshore transects are compared (see also Table 2). All stations show a general increase in Nd concentrations from the surface towards greater depth, ranging from 4.8 pmol/kg in surface waters to 24.1 pmol/kg in deep water samples. However, the increase is not always linear. Station 109 has nearly constant Nd concentrations around 8 pmol/kg in the upper 1500 m rising to 22 pmol/kg at the bottom. The northernmost station (St. 160) has a maximum concentration of 28.2 pmol/kg at 800 m water depth. The southernmost station (St. 30) close to the Peruvian coast shows an abrupt increase from 8 pmol/kg to 20 pmol/kg at a depth of 1000 m. Below that depth only a minor increase in Nd concentration was found down to about 5500 m. Some stations (109, 117, 134) show higher concentrations in the surface waters than in subsurface waters. Stations 152 and 159 (Table 2, data not shown in Fig. 3) show an increased concentration at 90 m (11 pmol/kg), respectively 100 m (20 pmol/kg) compared to similar depths in other profiles ($\sim$6 pmol/kg). The Nd isotope composition shows a wide range within the depth profiles of single stations overall ranging from $\varepsilon_{Nd}=-7$ to $\varepsilon_{Nd}=+2.7$. The mean Nd isotope composition of intermediate water masses between 200 m and 1500 m water depth ranges from $\varepsilon_{Nd}=-4$ (14°S) to $\varepsilon_{Nd}=-1.6$ (1°40′N) with no obvious differences between offshore and nearshore samples. Station 103 (9°S) shows the most heterogenic isotope signature of intermediate depth waters ranging from ($\varepsilon_{Nd}=-2.3$ to -7) with the most unradiogenic value ($\varepsilon_{Nd}=-7.0$) at 800 m water depth. During austral summer 2009, when the samples for this study were taken, the EUC encountered the western coast of South America at approximately 0°N to 1°N at a core depth of 90 m and then continued its flow southward. The presence of the SSCC, another subsurface water mass originating from the Central Pacific was observed between 5°S and 6°20′S with core depths of 100–200 m and 400–500 m, respectively (Czeschel et al., 2011). According to ADCP data (Czeschel et al., 2011) and the oxygen concentration of station 152 (85°50′W/Equator) and station 159 (85°50′W/1°20′N) are closest to those of the EUC at approximately 100 m water depth and show $\varepsilon_{Nd}=-1.8$ (10.5 pmol/kg) and $\varepsilon_{Nd}=-2.2$ (19.6 pmol/kg), respectively (Table 2, data not shown in Fig. 3). A water sample within the SSCC (St. 134, 100 m) shows an ε_{Nd} value of -2.2 (6.3 pmol/kg). The average ε_{Nd} value of these water masses originating in the Central Pacific is about $\varepsilon_{Nd}=-2.0$ (Fig. 3, dashed gray line). In relation to the radiogenic isotope signature of these zonal current bands (EUC/SSCC), the southern stations, in particular on the offshore transect show less radiogenic Nd isotope signatures compared to stations in the south.

3.2. Lateral distribution of Nd isotopes and concentrations in surface and deep water samples

Fig. 4 shows the variations of dissolved Nd isotope compositions and Nd concentrations together with hydrographic and nutrient data for surface and deep water samples (lowermost sample approximately 50 m above ground, only station 93 and station 117 were sampled at 500 m above the ground) for each station along the offshore and nearshore section between 16°S and 1°40′N. The surface waters (Figs. 2 and 4) are subdivided into 3 zones from south to north with following decreasing salinity: Subtropical Surface Water (STSW), Equatorial Surface Water (ESW) and Tropical Surface Water (TSW). The Nd isotope composition of surface waters becomes systematically more radiogenic towards the equator ranging from $\varepsilon_{Nd}=-3.3$ to $\varepsilon_{Nd}=+2.7$. The corresponding Nd concentrations increase from 5 pmol/kg at the southernmost stations (station 30 and station 93) to 12 pmol/kg at the northern end of the section (St. 160). Higher Nd concentrations are accompanied by increased silicic acid concentrations. Towards the equator the surface waters are less saline compared to the south. Offshore and nearshore surface waters show similar Nd isotope compositions and Nd concentrations, whereas the nearshore surface waters are characterized by lower surface temperatures (Fig. 4a).

Towards the north and similar to the surface water distribution, the Nd isotope composition of deep water samples becomes systematically more radiogenic ranging from $\varepsilon_{Nd}=-6.6$ at 14°S to $\varepsilon_{Nd}=-1.6$ at 1°40′N (Fig. 4b). The nearshore stations south of 14°S ($\varepsilon_{Nd}=-4$) show more radiogenic values compared to the offshore stations ($\varepsilon_{Nd}=-6$) mirroring lower oxygen concentrations. The highest potential temperature is observed in the north. The lowest Nd concentration (14 pmol/kg) in deep water samples close to the bottom is observed at the northernmost station, whereas Nd concentrations at the southern stations are approximately 20 pmol/kg.

4. Discussion

4.1. Controls of Nd isotopes and concentrations in surface and subsurface water masses

Surface waters in the study area of the EEP show a systematic trend towards more radiogenic ε_{Nd} values and higher Nd concentrations from south to north (Fig. 4a). This pattern is reflected by the hydrographic data given that continuously decreasing salinities are observed towards the equator (Fig. 4) due to enhanced rainfall (Wooster, 1959). The northernmost water masses represent the TSW range from $\varepsilon_{Nd}=+0.6$ to $+2.7$ and are sourced, among others, by the Panama Current (PaC), which is advected from the north (Figs. 1 and 4a). The Nd isotope composition of the PaC most likely originates from exchange with either volcanogenic particles in the water column or highly radiogenic shelf sediments along Central America ($\varepsilon_{Nd}=+2$ to $+6$, Jeandel et al., 2007). Tachikawa et al. (2004) and Lacan and Jeandel (2005) proposed that exchange between dissolved and

Table 2
Nd sample locations with depth, isotope composition of Nd (ε_{Nd}), Nd concentrations, potential temperature, potential density, salinity, silicic acid and oxygen concentrations.

	Depth (m)	ε_{Nd}	2sd	Nd (pmol/kg)	Pot. temp (°C)	Pot. density (kg/m^3)	Salinity (PSS-78)	$Si(OH)_4$ (μmol/kg)	Oxygen (μmol/kg)
St. 2	2	−2.7	0.3	5.8	14.79	25.99	35.26	0.35	219.8
10°S/80°W	101	−1.7	0.3	6.2	13.02	26.34	35.01	17.02	4.63
6296 m depth	498	−2.1	0.1	7.6	8.11	26.97	34.63	41.01	3.27
	991	−2.3	0.1	8.9	4.49	27.38	34.55	n.a	49.49
St. 30	3	−3.4	0.4	5.6	22.57	24.09	35.04	1.04	215.53
16°00'S/75°33'W	501	−2.9	0.5	7.8	7.28	27.04	34.57	37.54	15.94
6165 m depth	1011	−3.4	0.4	19.5	4.28	27.39	34.53	68.47	53.77
	3549	−4.3	0.5	18.9	1.51	27.76	34.69	134.49	124.36
	4571	−4.9	0.5	22.1	1.36	27.78	34.70	121.29	141.94
	5494	−4.5	0.5	24.1	1.31	27.78	34.70	126.5	142
St. 78	2	−2.6	0.4	5.9	19.54	24.83	34.93	n.a	219.54
14°00'S/77°03'W	199	−2.3	0.4	6.8	12.37	26.44	34.89	n.a	2.99
3026 m depth	498	−2.5	0.4	7.7	7.74	26.99	34.59	n.a	9.08
	1999	−3.2	0.3	11.8	2.15	27.67	34.64	n.a	103.38
	2498	−4.7	0.3	14.5	1.70	27.73	34.67	n.a	131.73
	2986	−3.6	0.3	17.0	1.55	27.75	34.68	n.a	132.55
St. 93	3	−2.3	0.2	5.0	24.72	23.82	35.52	0.22	221.17
14°00'S/85°50'W	161	−4.8	0.4	7.4	12.52	26.34	34.82	23.71	2.91
4579 m depth	1007	−3.2	0.4	8.9	4.32	27.39	34.54	79.50	57.98
	2003	−2.3	0.3	11.8	2.16	27.67	34.64	130.85	105.82
	3004	−3.1	0.3	16.9	1.60	27.74	34.68	138.71	132.76
	4036	−6.6	0.3	21.7	1.44	27.76	34.69	127.87	153.06
St. 103	2	−3.3	0.3	4.8	26.75	23.19	35.52	0.77	215.51
9°00'S/85°50'W	152	−2.3	0.1	6.1	13.06	26.34	34.95	21.54	10.38
4299 m depth	221	−2.5	0.3	6.1	12.31	26.46	34.91	21.74	33.63
	800	−7.0	0.4	8.0	5.48	27.26	34.55	66.41	33.98
	1501	−4.7	0.1	10.2	2.85	27.58	34.61	121.64	83.24
	2501	−2.2	0.4	14.4	1.74	27.73	34.67	147.57	118.26
	4292	−4.4	0.1	21.0	1.45	27.76	34.69	138.86	146.45
St. 109	2	−0.4	0.1	7.9	25.40	22.83	34.49	1.03	214.99
3°35'S/85°50'W	151	−3.5	0.2	6.3	13.50	26.26	34.96	19.57	46.40
3261 m depth	499	−2.6	0.1	8.1	8.13	26.97	34.64	46.14	8.60
	701	−1.1	0.2	9.4	6.22	27.19	34.57	61.00	22.08
	1501	−1.8	0.3	8.1	3.13	27.56	34.61	118.06	80.04
	3201	−4.3	0.1	21.6	1.54	27.75	34.68	143.63	134.31
St. 117	2	−1.5	0.2	7.8	22.53	23.66	34.4567	2.69	195.24
3°35'S/82°00'W	150	−2.3	0.1	6.6	13.62	26.24	34.9622	19.18	47.08
4084 m depth	398	−2.8	0.1	8.4	9.06	26.87	34.6897	41.61	6.05
	1487	−3.2	0.8	11.1	3.09	27.57	34.6103	121.07	79.61
	2473	−3.9	0.2	15.9	1.76	27.73	34.6696	145.6	116.68
	3453	−3.7	0.2	20.4	1.53	27.75	34.6815	144.08	132.58
St. 134	2	−0.2	0.4	9.0	26.90	22.30	34.39	1.52	218.81
6°00'S/85°50'W	99	−2.2	0.4	6.3	13.83	26.21	34.98	18.20	28.77
4113 m depth	745	−1.7	0.4	8.1	5.77	27.23	34.56	63.34	34.78
	3942	−3.5	0.3	18.7	1.50	27.76	34.68	141.66	136.49
St. 152	3	0.6	0.1	8.6	26.06	21.97	33.61	1.69	212.23
Equator/85°50'W	90	−1.8	0.1	10.5	14.01	26.17	34.98	15.74	87.72
2907 m depth									
St. 159	1	1.1	0.1	9.8	24.33	22.00	32.95	4.16	189.02
1°20'N/85°50'W	52	−1.8	0.3	5.9	14.72	26.04	35.01	13.70	94.68
2977 m depth	99	−2.2	0.4	19.6	14.03	26.17	34.98	15.30	92.38
St. 160	4	2.7	0.4	12.4	25.01	21.55	32.63	7.07	189.74
1°40'N/85°50'W	199	−2.5	0.4	14.2	12.99	26.33	34.91	20.82	51.80
2607 m depth	795	−1.6	0.4	28.2	5.81	27.24	34.57	67.34	43.94
	1488	−0.8	0.4	11.7	3.04	27.57	34.61	122.27	78.16
	2607	−1.6	0.3	14.0	1.87	27.72	34.67	150.92	104.48

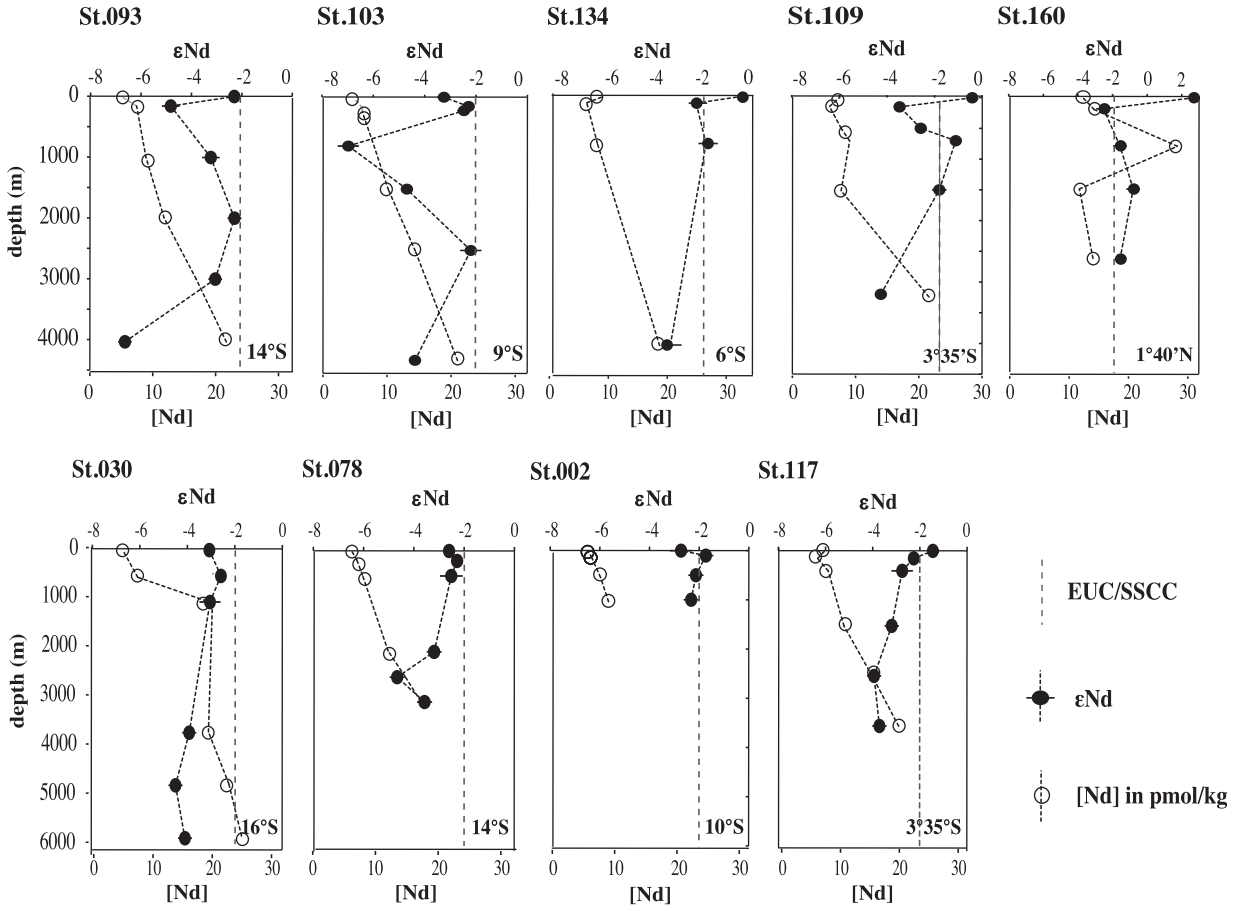

Fig. 3. Nd isotope composition (ε_{Nd}, filled black circles) and Nd concentrations in pmol/kg (open circles) of 9 stations. Offshore stations along the 85°50′W are shown in the upper part of the graph. Nearshore stations (100–200 km off the coast) are shown in the lower part. Stations 152 and 159, for which only 2 water depths were sampled are not shown. The dashed gray line indicates the isotope signature of the EUC/SSCC encountered from stations 152, 159 and 134. Please note the different scale for the ε_{Nd} values at station 160.

particulate phases significantly contributes to the dissolved isotopic signal of a water mass.

ESW from offshore stations shows a characteristic Nd isotope composition of approximately $\varepsilon_{Nd} = -0.3$. The nearshore station at 3°35′S with its distinct Nd isotope signature of $\varepsilon_{Nd} = -1.5$ is either more influenced by surface currents originating in the south or by upwelled waters which have received their isotopic fingerprints from the shelf margin. Surface waters south of 8°S show higher salinities and are generally referred to STSW, which is characterized by isotope signatures between $\varepsilon_{Nd} = -3.3$ and $\varepsilon_{Nd} = -2.3$. These water masses are clearly influenced by less radiogenic surface currents, such as the POC, PCC and the SEC (Fig. 1a) which originate in the south and are transported westward due to persistent easterly trade winds.

Surface waters in the northern part of the study area show more than twice the Nd concentrations (12 pmol/kg) compared to surface waters in the south (5 pmol/kg, Fig. 4a). High concentrations in the north could be a result of the incoming PaC. Its pathway along Central America makes it prone to inputs from dissolution of easily weatherable volcanogenic particles, which is also supported by the highly radiogenic Nd isotope signatures in these samples. Furthermore lower Nd concentrations in the south could be the result of Nd-depleted westward flowing water masses, such as the POC and PCC originating in high productivity areas along the Peruvian and Chilean shelves (Chavez and Barber, 1987; Chavez and Messié, 2009), which goes along with high biogenic particle density. This particle density can cause enhanced scavenging of dissolved Nd. Furthermore the low dissolved Nd concentrations correlate well with low silicic acid concentrations (Fig. 4a). As diatoms are dominating the phytoplankton in upwelling areas (Estrada and Blasco, 1985), it is most likely that Nd is scavenged by the large surfaces of the diatoms. In the Atlantic sector of the Southern Ocean a similar explanation for the strong correlation between Nd and silicic acid concentration has been proposed by Stichel et al. (2012). During the cruise in February 2009 the core of the EUC, which could be identified due to ADCP data and elevated oxygen concentrations (~90 μmol) was found immediately north of the equator at water depths between 80 m and 100 m (Czeschel et al., 2011). Hydrographic parameters at stations 152 and 159 at 85°50′W at the equator are closest to those of the EUC at approximately 100 m water depth and show $\varepsilon_{Nd} = -1.8$ and $\varepsilon_{Nd} = -2.2$, respectively. These values are in good agreement with data from Lacan and Jeandel (2001) which obtained $\varepsilon_{Nd} = -1.6$ for the core of the EUC at 140°W. They suggested that this water mass obtains its radiogenic signature, when the AAIW passes the, which consists of easily weatherable island arc rocks, before flowing eastward. Nd concentrations of the EUC (Sts. 152 and 159) are 2–3 times higher (11 pmol/kg; respectively 20 pmol/kg) compared to similar depths at other stations (~6 pmol/kg). This agrees with investigation by Slemons et al. (2010) and Kaupp et al. (2011) who also reported elevated dissolved iron and aluminum concentrations in the EUC, most likely caused by sediment resuspension and

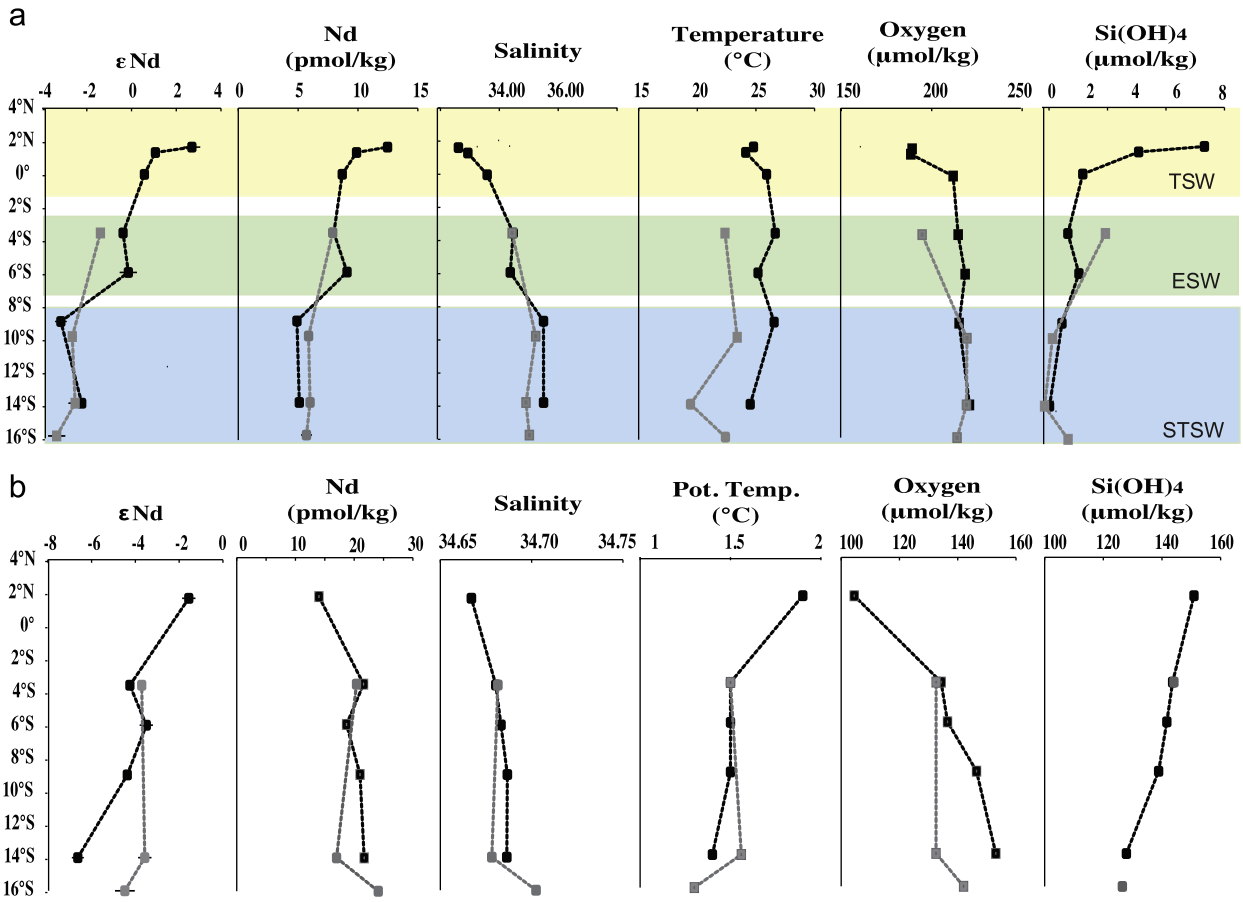

Fig. 4. For each station the surface water (a) and deep water (b) ε_{Nd}, Nd concentration (pmol/kg), salinity (PSU), potential temperature (°C), oxygen and silicic acid concentration (µmol/kg) are plotted against latitude. The black line marks the 85°50′W transect, the gray line marks the nearshore transect. Color shaded areas in the upper plot represent the different surface water masses (TSW: Tropical Surface Water; ESW: Equatorial Surface Water; STSW: Subtropical Surface Water). All deep water samples were sampled below 3000 m, only the northernmost station (St. 160) was sampled at 2600 m water depth.

particle release processes in the source area of the zonal current band near Papua New Guinea, which was also shown to be a source of dissolved REEs (Sholkovitz et al., 1999). The SSCC, another subsurface water mass originating from the Central Pacific influencing the intermediate depth waters of the study area, was observed between 5°S and 6°20′S with core depths of 100–200 m and 400–500 m, respectively. The SSCC (St. 134, 100 m) shows a $\varepsilon_{Nd}=-2.2$, similar to the EUC. These zonal current bands are feeding the PCUC, the main source water mass for the upwelling, with up to 30% of its volume (Montes et al., 2010). Therefore the PCUC should accordingly be influenced by this radiogenic isotope composition. The hydrographic data, characterized by a salinity minimum in the subsurface for St. 93 and St. 30 show a clear influence of SAAW, which originates in the south (Fig. 2). No water sample was taken from exactly the depth where the peak of the salinity minimum was located. Only station 93 shows a less radiogenic signature ($\varepsilon_{Nd}=-4.8$) at a depth of 160 m, which corresponds to the lower part of the salinity minimum.

In summary, highly radiogenic surface and subsurface water masses of the EEP are not only a result of advection of water masses from the Central Pacific with their radiogenic isotope signature but also local sources, such as the Central American coast seem to play an important role for the surface water Nd isotopic signature. This is clearly indicated by the highly radiogenic Nd isotope compositions of the water masses transported to the study area by the Panama Current (Fig. 1a).

4.2. Intermediate water masses

Intermediate water masses between 200 m and 1500 m depth show a relatively wide range in their isotopic composition from $\varepsilon_{Nd}=-2.1$ to $\varepsilon_{Nd}=-7$, with a trend to more radiogenic mean values towards the north ($\varepsilon_{Nd}=-4$ (14°S) to $\varepsilon_{Nd}=-1.6$ (1°40′N)). For a simple mixture of NPIW ($\varepsilon_{Nd}=-3.4$ to $\varepsilon_{Nd}=-2.7$; Amakawa et al., 2004, 2009) and AAIW ($\varepsilon_{Nd}=-6.0$ to $\varepsilon_{Nd}=-7.0$; Stichel et al., 2012) the intermediate water Nd isotope compositions are too radiogenic. This is consistent with the study of Bostock et al. (2010) who suggested that a mixture of AAIW and NPIW does not directly form the EqPIW. This is supported for example by radiocarbon data which indicate an influence by lateral advection of an older deeper water mass. Station 103 shows a quite unradiogenic Nd isotope composition ($\varepsilon_{Nd}=-7$) at 800 m, which is suggesting an admixture of a southern water mass, most likely AAIW, which is transported westward with the subtropical gyre. However this is not clearly supported by the hydrographic data. The Nd profiles show relatively heterogeneous isotope compositions with highly radiogenic values even at deeper water masses (e.g. St. 103, 2500 m, $\varepsilon_{Nd}=-2.2$) that cannot always be explained by mixtures of specific water masses most likely due to the fact that the EEP is a highly dynamic system, in which also mesoscale eddies play an important role for the vertical and horizontal mixing processes (Chaigneau et al., 2008).

This is also reflected by station 160, which shows a peak Nd concentration (30 pmol/kg) at 800 m depth (Fig. 3). Such concentration peaks may be explained by intrusions of water masses

that obtained their high Nd concentrations on the shelf before being transported offshore. Rickli et al. (2009) found a similar concentration peak in the Bay of Biscay accompanied by an increased dissolved iron concentration that was also ascribed to such an intrusion (Laës et al., 2003). Elevated dissolved iron concentration in the water column can derive from water masses that have been in contact with shelf sediments as iron is readily dissolved and released from sub-oxic or anoxic sediments, such as those on the Peruvian shelf (Landing and Bruland, 1987; Bruland et al., 2005).

4.3. Deep and bottom waters

Deep and bottom water samples show the least radiogenic neodymium isotope signatures ($\varepsilon_{Nd}=-6.6$) at the southernmost station at 85°50′W with a clear trend to more radiogenic values in the north ($\varepsilon_{Nd}=-1.6$, Fig. 4b). The deep water masses along the offshore transect in the south are less radiogenic and coincide with higher oxygen and lower silicic acid concentrations indicating a larger proportion of LCDW ($\varepsilon_{Nd}=-8.5$, Stichel et al., 2012) compared to the nearshore water masses. Given that LCDW does not spread into all areas of the Pacific (Johnson and Toole, 1993), admixture of NPDW is also expected ($\varepsilon_{Nd}=-3.8$, Piepgras and Jacobsen, 1988). In order to calculate the fractions of water masses of northern and southern origin contributing to the deep water in the EEP we assumed simple mixing of NPDW with LCDW, which is described by the following equation:

$$\varepsilon Nd_{mix}=\left(\frac{(\varepsilon Nd_1\times[Nd]_1\times f)+(\varepsilon Nd_2\times[Nd]_2\times(1-f))}{[Nd]_1\times f+[Nd]_2\times(1-f)}\right)$$

εNd_{mix} is the isotope composition of the mixed water mass. εNd_1 and εNd_2 represent the isotope composition of the 2 endmembers, $[Nd]_1$ and $[Nd]_2$ are the corresponding concentrations and f the percentage of the respective endmember.

For the mixing line (Fig. 5) we applied Nd isotope and concentration data from Piepgras and Jacobsen (1988) for NPDW at 24°25′N and 141°85′E and from Stichel et al. (2012) for LCDW (57°37′S, 60°50′W). It is clear that this is an oversimplification but given the similarity of various water profiles in the respective source areas, the choice of these numbers is justified to achieve first order estimates.

The measured Nd isotope ratios and concentrations in the deep waters of the EEP are not in good agreement with the mixing line between the NPDW and LCDW (Fig. 5). Dissolved Nd concentrations in EEP deep waters are obviously depleted; respectively the Nd isotope compositions are too radiogenic. So far no other water profiles from the Pacific Ocean have shown concentrations in deep waters similarly low to those obtained in this study. Nd concentrations in deep waters (below 3000 m) of the North and Central Pacific generally show concentrations of 40–60 μmol/kg (Vance et al., 2004; Piepgras and Wasserburg, 1982; Piepgras and Jacobsen, 1988; Amakawa et al., 2009), which are more than twice as high as in the EEP. A possible explanation could be that a different water mass with a more radiogenic Nd isotope signature and low Nd concentrations is admixed and the 2 endmember mixing is incorrect. But a more likely explanation for the diminished concentration is efficient scavenging of dissolved Nd by particles. Due to intense upwelling of nutrient rich subsurface waters the EEP is characterized by high primary productivity (Pennington et al., 2006) and therefore high particle densities. The sinking biogenic particles will adsorb the dissolved Nd and, as already mentioned, it is particularly the large phytoplankton species such as diatoms, which dominate the biogenic particles in the study area (Estrada and Blasco, 1985). In support of this, a modeling study by Arsouze et al. (2009) suggested that particle size and the resulting sinking velocity will have a significant influence on the dissolved Nd concentration as well as the Nd isotope composition in the deep water, when the particles are remineralized with depth. A comparison to modeled data by Rempfer et al. (2011), which shows Nd concentrations in the study area between 28 pmol/kg and 36 pmol/kg (below 3000 m) compared to the measured Nd concentrations of this study (~20 pmol/kg) also suggests the presence of highly efficient removal processes in the EEP which were not included in the model parameters.

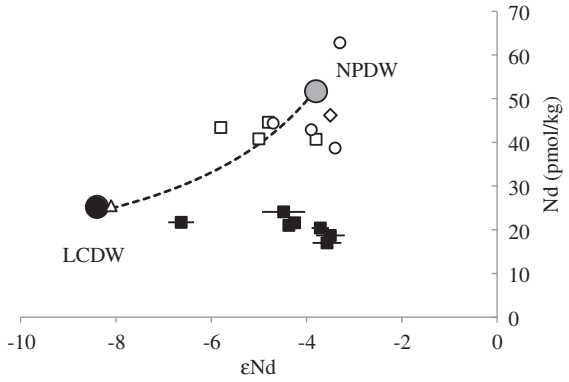

Fig. 5. The plot shows the mixing line (dashed line) between LCDW (black dot) and NPDW (gray dot) for Nd concentration (pmol/kg) against Nd isotope composition (ε_{Nd}). Black squares indicate deep water samples in the study area (below 3000 m). Open symbols indicate water samples below 3000 m water depth from the North and Central Pacific Ocean according to published data (Piepgras and Wasserburg, 1982 (open triangle); Amakawa et al., 2009 (open squares), Piepgras and Jacobsen, 1988 (open circles), Vance et al., 2004 (open diamond). Endmember values for Nd isotope signatures and Nd concentrations of NPDW and LCDW are taken from Piepgras and Jacobsen (1988); $\varepsilon_{Nd}=-3.8$, [Nd]=51.7 pmol/kg, Stichel et al. (2012); $\varepsilon_{Nd}=-8.5$, [Nd]=25.3 pmol/kg).

At the same time, deep water masses at the northernmost station (St. 160, Fig. 3) are highly radiogenic in their Nd isotope composition, even at a depth of 1500 m ($\varepsilon_{Nd}=-0.8$), respectively 2600 m ($\varepsilon_{Nd}=-1.6$). These radiogenic values in the north are similar to data obtained from a ferromangenese crust that incorporated its isotopic signature from bottom waters at approximately 14°N off the Mexican coast ($\varepsilon_{Nd}=-2.5$, Frank et al., 1999). One possible explanation for the radiogenic Nd isotope signatures in the deep waters is intense exchange processes with the nearby continental margin, which is characterized by highly radiogenic Nd isotope values in this area ($\varepsilon_{Nd}=\sim+10$, Jeandel et al., 2007). Many authors have suggested that boundary exchange processes with continental margins play an important, if not the dominant role for the dissolved Nd isotope composition of seawater (Lacan and Jeandel, 2005; Arsouze et al., 2007, 2009), but also exchange processes with deep-sea sediments may exert some influence.

Another possible explanation is vertical transport of particles with radiogenic isotope signatures from surface waters to the deep ocean. Surface waters in the northern part of the study area are characterized by highly radiogenic values of $\varepsilon_{Nd}=0$ to $\varepsilon_{Nd}=+3$, which have probably been controlled by partial dissolution of particles. When these particles sink to the bottom and keep releasing Nd, this will also influence the dissolved Nd isotope signal of the deep waters. Vertical processes can thus explain the radiogenic Nd isotope values of deep water masses at the northern stations but not their diminished concentrations. Our data clearly suggest that not only exchange but also net removal of Nd in the EEP water column must occur during the scavenging processes for example by biogenic particles. The removal can be considered very efficient given that the anoxic sediments underlying the OMZ off Peru are expected to represent

an additional source of REEs (Elderfield and Sholkovitz, 1987; Haley et al., 2004) and other redox-sensitive metals, such as iron (Landing and Bruland, 1987; Bruland et al., 2005). The above combined effects best explain why the deep water masses in the Eastern Pacific basin do not fit on a hypothetical mixing line between LCDW and NPDW (Fig. 5).

The general agreement of the Nd isotope distribution with that of the major water masses supports the applicability of Nd as a proxy for present and past ocean circulation. Zonal surface and subsurface currents, which transport oxygen-rich water to the upwelling area, are clearly traceable by their specific radiogenic Nd isotope compositions. By extracting the Nd isotope composition of past water masses involved in the Peruvian upwelling this information can be used to reconstruct the import of oxygen-rich waters to the shelf regions and therefore to determine changes in the strength of the OMZ caused by changes in advective supply of oxygen. However, the results of our study also demonstrate that in areas with high particle fluxes and prevalence of easily weatherable phases, such as volcanogenic particles, the dissolved Nd isotope signal of the waters can be influenced. This has to be taken into account for the interpretation of paleo records in shelf regions, as well as for the reconstruction of deep water mass mixing.

5. Conclusions

This study presents the first full water column distributions of dissolved Nd isotopes and Nd concentrations in the EEP. Zonal current bands from the Central Pacific, like the EUC and the SSCC providing oxygen-rich water masses are clearly traceable by distinctly radiogenic Nd isotope compositions ($\varepsilon_{Nd} = -2$), which can be used to reconstruct the evolution of advective import of oxygen-rich water masses into the coastal upwelling system and the OMZ off Peru. More radiogenic Nd isotope signatures in the northern part of the study area indicate the advection of Central Pacific Water masses into intermediate water depths of the EEP. The deep water Nd isotope signatures in all profiles reflect the mixture between sources in the Southern Ocean and the North Pacific except the northernmost station from the Panama Basin.

There is, however, also clear evidence for non-conservative effects. Surface water masses show a trend towards more radiogenic values in the north coupled to higher Nd concentrations, which is obviously caused by particle exchange. Deep and bottom waters in the northern part of the study area are significantly depleted in their Nd concentration and at the same time show more radiogenic isotopic signatures than expected from mixing between NPDW and LPDW. To explain these observations dissolved Nd must be scavenged resulting in a net removal from the water column, most likely by the large amounts of sinking biogenic particles. At the same time, some of the scavenged Nd must be released to the deep and bottom waters, which is documented by highly radiogenic Nd isotope compositions in the entire water column in the northern part of the study area. These radiogenic Nd isotope signatures may at least partly be the result of the transport of volcanic particles from surface waters to the deep ocean, where partial dissolution and release of radiogenic Nd occurs. In addition, exchange processes with the shelf sediments at the Peruvian margin may also have contributed to the observed dissolved Nd isotope distribution.

Acknowledgments

This work is a contribution of the Sonderforschungsbereich 754 "Climate—Biogeochemistry Interactions in the Tropical Ocean" (www.sfb754.de), which is funded by the Deutsche Forschungsgemeinschaft. Special thanks go to the crew of the R/V Meteor.

References

Amakawa, H., Alibo, D.S., Nozaki, Y., 2000. Nd isotopic composition and REE pattern in the surface waters of the eastern Indian Ocean and its adjacent seas. Geochim. Cosmochim. Acta 64, 1715–1727.

Amakawa, H., Nozaki, Y., Alibo, D.S., Zhang, J., Fukugawa, K., Nagai, H., 2004. Neodymium isotopic variations in Northwest Pacific waters. Geochim. Cosmochim. Acta 68, 715–727.

Amakawa, H., Sasaki, K., Ebihara, M., 2009. Nd isotopic composition in the central North Pacific. Geochim. Cosmochim. Acta 73, 4705–4719.

Arsouze, T., Dutay, J., Lacan, F., Jeandel, C., 2007. Modeling the neodymium isotopic composition with a global ocean circulation model. Chem. Geol. 239, 165–177.

Arsouze, T., Dutay, J.-C., Lacan, F., Jeandel, C., 2009. Reconstructing the Nd oceanic cycle using a coupled dynamical–biogeochemical model. Biogeosciences 6, 2829–2846.

Ayon, P., Criales-Hernandez, M.I., Schwamborn, R., Hirche, H., 2008. Zooplankton research off Peru: a review. Prog. Oceanogr. 79, 238–255.

Barrat, J.A., Keller, F., Amossé, J., Taylor, R.N., Nesbitt, R.W., Hirata, T., 1996. Determination of Rare Earth Elements in sixteen silicate reference samples by ICP-MS after Tm addition and ion exchange separation. Geostand. Geoanal. Res. 20, 133–139.

Bostock, H.C., Opdyke, B.N., Williams, M.J.M., 2010. Characterising the intermediate depth waters of the Pacific Ocean using $\delta^{13}C$ and other geochemical tracers. Deep-Sea Res. I 57, 847–859.

Brink, K., Halpern, D., Huyer, A., Smith, R.L., 1983. The physical environment of the Peruvian upwelling system. Prog. Oceanogr. 12, 285–305.

Bruland, K., Rue, E., Smith, G., Ditullio, G., 2005. Iron, macronutrients and diatom blooms in the Peru upwelling regime: brown and blue waters of Peru. Mar. Chem. 93, 81–103.

Chaigneau, A., Gizolme, A., Grados, C., 2008. Mesoscale eddies off Peru in altimeter records: identification algorithms and eddy spatio-temporal patterns. Prog. Oceanogr. 79, 106–119.

Chavez, F.P., Barber, R.T., 1987. An estimate of new production in the equatorial Pacific. Deep-Sea Res. I 34, 1229–1243.

Chavez, F.P., Messié, M., 2009. A comparison of Eastern Boundary Upwelling Ecosystems. Prog. Oceanogr. 83, 80–96.

Czeschel, R., Stramma, L., Schwarzkopf, F.U., S.B, Funk, A., Karstensen, J., 2011. Mid-depth circulation of the eastern tropical South Pacific and its link to the oxygen minimum zone. J. Geophys. Res. 116, C01015, http://dx.doi.org/10.1029/2010JC006565.

Elderfield, H., Greaves, M.J., 1982. The rare earth elements in seawater. Nature 296, 214–219.

Elderfield, H., Sholkovitz, E., 1987. Rare earth elements in the pore waters of reducing nearshore sediments. Earth Planet. Sci. Lett. 82, 280–288.

Elderfield, H., Upstill-Goddard, R., Sholkovitz, E., 1989. The rare earth elements in rivers, estuaries, and coastal seas and their significance to the composition of ocean waters. Geochim. Cosmochim. Acta 54, 971–991.

Estrada, M., Blasco, D., 1985. Phytoplankton assembledges in coastal upwelling areas. In: Bas, C., Margalef, R., Rubies, P. (Eds.), Simposio Internacional Sobre Las Areas de Afloramiento Mas Importantes del Oeste Africano (Cabo Blanco y Banguela). Instituto de Investigaciones Pesqueras, Barcelona, pp. 379–402.

Fiedler, P., Talley, L., 2006. Hydrography of the eastern tropical Pacific: a review. Prog. Oceanogr. 69, 143–180.

Frank, M., Reynolds, B.C., O'Nions, R.K., 1999. Nd and Pb isotopes in Atlantic and Pacific water masses before and after closure of the Panama gateway. Geology 27, 1147–1150.

Frank, M., 2002. Radiogenic isotopes: tracers of past ocean circulation and erosional input. Rev. Geophys. 40, 1001, http://dx.doi.org/10.1029/2000RG000094.

German, C.R., Klinkhammer, G.P., Edmond, J.M., Mitra, A., Elderfield, H., 1990. Hydrothermal scavenging of rare-earth elements in the ocean. Nature 345, 516–518.

Goldstein, S., O'Nions, R.K., Hamilton, P., 1984. A Sm–Nd isotopic study of atmospheric dusts and particulates from major river systems. Earth Planet. Sci. Lett. 70, 221–236.

Goldstein, S.J., Jacobsen, S.B., 1988. REE in the Great Whale River estuary, northwest Quebec. Earth Planet. Sci. Lett. 88, 241–252.

Grasshoff, K., Kremling, K., Ehrhardt, M., 1999. Methods of Seawater Analysis. Verlag Chemie, Weinheim (pp. 159–228).

Haley, B.A., Klinkhammer, G.P., McManus, J., 2004. Rare earth elements in pore waters of marine sediments. Geochim. Cosmochim. Acta 68, 1265–1279.

Halliday, N., Davidson, P., Holden, P., Owen, M., Olivarez, M., 1992. Metalliferous sediments and the scavenging residence time of Nd near hydrothermal vents. Geophys. Res. Lett. 19, 761–764.

Henry, F., Jeandel, C., Dupré, B., Minster, J.-F., 1994. Particulate and dissolved Nd in the western Mediterranean Sea: sources, fate and budget. Mar. Chem. 45, 283–305.

Heumann, K.G., 1992. Isotope dilution mass spectrometry (IDMS) of the elements. Mass Spectrom. Rev. 11, 41–67.

Huyer, A., Smith, R.L., Paluszkiewicz, T., 1987. Coastal upwelling off Peru during normal and El Niño times, 1981–1984. J. Geophys. Res. 92 (C13), 14297–14307.
Jacobsen, S.B., Wasserburg, G.J., 1980. Sm–Nd isotopic evolution of chondrites. Earth Planet. Sci. Lett. 50, 139–155.
Jeandel, C., Bishop, J.K., Zindler, A., 1995. Exchange of neodymium and its isotopes between seawater and small and large particles in the Sargasso Sea. Geochim. Cosmochim. Acta 59, 535–547.
Jeandel, C., Arsouze, T., Lacan, F., Techine, P., Dutay, J., 2007. Isotopic Nd compositions and concentrations of the lithogenic inputs into the ocean: a compilation, with an emphasis on the margins. Chem. Geol. 239, 156–164.
Johnson, G., Toole, J., 1993. Flow of deep and bottom waters in the Pacific at 10°N. Deep-Sea Res. I 40, 371–394.
Jones, K.M., Khatiwala, S.P., Goldstein, S.L., Hemming, S.R., van de Flierdt, T., 2008. Modeling the distribution of Nd isotopes in the oceans using an ocean general circulation model. Earth Planet. Sci. Lett. 272, 610–619.
Karstensen, J., Ulloa, O., 2008. The Peru–Chile Current System. Encyclopedia of Ocean Sciences, 2nd edition online.
Kaupp, L.J., Measures, C.I., Selph, K.E., Mackenzie, F.T., 2011. The distribution of dissolved Fe and Al in the upper waters of the Eastern Equatorial Pacific. Deep-Sea Res. II 58, 296–310 (Elsevier).
Kawabe, M., Fujio, S., 2010. Pacific ocean circulation based on observation. J. Oceanogr. 66, 389–403.
Kessler, W., 2006. The circulation of the eastern tropical Pacific: a review. Prog. Oceanogr. 69, 181–217.
Klinkhammer, G.P., Elderfield, H., Hudson, A., 1983. Rare earth elements in seawater near hydrothermal vents. Nature 305, 185–187.
Lacan, F., Jeandel, C., 2001. Tracing Papua New Guinea imprint on the central Equatorial Pacific Ocean using neodymium isotopic compositions and Rare Earth Element patterns. Earth Planet. Sci. Lett. 186, 497–512.
Lacan, F., Jeandel, C., 2005. Neodymium isotopes as a new tool for quantifying exchange fluxes at the continent–ocean interface. Earth Planet. Sci. Lett. 232, 245–257.
Laës, A., Blain, S., Laan, P., Achterberg, E.P., Sarthou, G., de Baar, H.J.W., 2003. Deep dissolved iron profiles in the eastern North Atlantic in relation to water masses. Geophys. Res. Lett. 30, 1902, http://dx.doi.org/10.1029/2003GL017902.
Landing, W., Bruland, K., 1987. The contrasting biogeochemistry of iron and manganese in the Pacific Ocean. Geochim. Cosmochim. Acta 51, 29–43.
Le Fèvre, B., Pin, C., 2005. A straightforward separation scheme for concomitant Lu–Hf and Sm–Nd isotope ratio and isotope dilution analysis. Anal. Chim. Acta 543, 209–221.
Montes, I., Colas, F., Capet, X., Schneider, W., 2010. On the pathways of the equatorial subsurface currents in the eastern equatorial Pacific and their contributions to the Peru–Chile undercurrent. J. Geophys. Res. 115, C09003 http://dx.doi.org/10.1029/2009JC005710.
Oka, A., Hasumi, H., Obata, H., Gamo, T., Yamanaka, Y., 2009. Study on vertical profiles of rare earth elements by using an ocean general circulation model. Global Biogeochem. Cycles 23, GB4025, http://dx.doi.org/10.1029/2008GB003353.
Piepgras, D.J., Wasserburg, G.J., Dasch, E.J., 1979. The isotopic composition of Nd in different water masses. Earth Planet. Sci. Lett. 45, 223–236.
Piepgras, D.J., Wasserburg, G.J., 1982. Isotopic composition of neodymium in waters from the Drake passage. Science 217, 207–217.
Piepgras, D.J., Jacobsen, S.B., 1988. The isotopic composition of neodymium in the North Pacific. Geochim. Cosmochim. Acta 52, 1373–1381.
Pennington, J.T., Mahoney, K., Kuwahara, V., Kolber, D., Calienes, R., Chavez, F., 2006. Primary production in the eastern tropical Pacific: a review. Prog. Oceanogr. 69, 285–317.
Penven, P., Echevin, V., Pasapera, J., Colas, F., Tam, J., 2005. Average circulation, seasonal cycle, and mesoscale dynamics of the Peru Current System: a modeling approach. J. Geophys. Res. 110, C10021, http://dx.doi.org/10.1029/2005JC002945.
Rempfer, J., Stocker, T.F., Joos, F., Dutay, J.-C., Siddall, M., 2011. Modeling Nd isotopes with a coarse resolution ocean circulation model: sensitivities to model parameters and source/sink distributions. Geochim. Cosmochim. Acta 75, 5927–5950.
Rickli, J., Frank, M., Halliday, A.N., 2009. The hafnium–neodymium isotopic composition of Atlantic seawater. Earth Planet. Sci. Lett. 280, 118–127.
Shimizu, H., Tachikawa, K., Masuda, A., Nozaki, Y., 1994. Cerium and neodymium isotope ratios and REE patterns in seawater from the North Pacific Ocean. Geochim. Cosmochim. Acta 58, 323–333.
Sholkovitz, E.R., Elderfield, H., Szymczak, R., Casey, K., 1999. Island weathering: river sources of rare earth elements to the Western Pacific Ocean. Mar. Chem. 68, 39–57.
Siddall, M., Khatiwala, S., van de Flierdt, T., Jones, K., Goldstein, S., Hemming, S., Anderson, R.F., 2008. Towards explaining the Nd paradox using reversible scavenging in an ocean general circulation model. Earth Planet. Sci. Lett. 274, 448–461.
Silva, N., Rojas, N., Fedele, A., 2009. Water masses in the Humboldt Current System: properties, distribution, and the nitrate deficit as a chemical water mass tracer for Equatorial Subsurface Water off Chile. Deep-Sea Res. II 56, 1004–1020.
Slemons, L.O., Murray, J.W., Resing, J., Paul, B., Dutrieux, P., 2010. Western Pacific coastal sources of iron, manganese, and aluminum to the Equatorial Undercurrent. Global Biogeochem. Cycles 24, GB3024, http://dx.doi.org/10.1029/2009GB003693.
Stichel, T., Frank, M., Rickli, J., Haley, B.A., 2012. The hafnium and neodymium isotope composition of seawater in the Atlantic sector of the Southern Ocean. Earth Planet. Sci. Lett. 317–318, 212–294.
Strub, P.T., Mesías, J.M., Montecino, V., Rutllant, J., 1998. Coastal ocean circulation off western South America. Sea 11, 273–313.
Tachikawa, K., Jeandel, C., Roy-Barman, M., 1999. A new approach to the Nd residence time in the ocean: the role of atmospheric inputs. Earth Planet. Sci. Lett. 170, 433–446.
Tachikawa, K., Athias, V., Jeandel, C., 2003. Neodymium budget in the modern ocean and paleo-oceanographic implications. J. Geophys. Res. 108, 3254 http://dx.doi.org/10.1029/1999JC000285.
Tachikawa, K., Roy-Barman, M., Michard, Thouron, D., Yeghicheyan, D., Jeandel, C., 2004. Neodymium isotopes in the Mediterranean Sea: comparison between seawater and sediment signals. Geochim. Cosmochim. Acta 68, 3095–3106.
Talley, L., 1993. Distribution and formation of North Pacific intermediate water. J. Phys. Oceanogr. 23, 517–538.
Talley, L., 1999. Some aspects of ocean heat transport by shallow, intermediate and deep overturning circulation. In: Clark, Webb, Keigwin (Eds.), Mechanisms of Global Climate change at Millenial Time Scales, Geophysical Monograph Series, vol. 112. American Geophysical Union, pp. 1–22.
Tanaka, T., Togashi, S., Kamioka, H., Amakawa, H., Kagami, H., Hamamoto, T., Yuhara, M., Orihasi, Y., Yoneda, S., Shimizu, H., Kunimaru, T., Takahashi, K., Yanagi, T., Nakano, T., Fujimaki, H., Shinjo, R., Asahara, Y., Tanimizu, M., Dragusanu, C., 2000. JNdi-1: a neodymium isotopic reference in consistency with LaJolla neodymium. Chem. Geol. 168, 279–281.
Toggweiler, J.R., Dixon, K., Broecker, W.S., 1991. The Peru Upwelling and the ventilation of the South Pacific thermocline. J. Geophys. Res. 96 (C11), 20467–20497.
Vance, D., Scrivner, A.E., Beney, P., Staubwasser, M., Henderson, G.M., Slowey, N.C., 2004. The use of foraminifera as a record of the past neodymium isotope composition of seawater. Paleoceanography 19, PA2009, http://dx.doi.org/10.1029/2003PA000957.
Wijffels, S., Toole, J., Bryden, H., Fine, R., Jenkins, W., Bullister, J., 1996. The water masses and circulation at 10°N in the Pacific. Deep-Sea Res. I 43, 501–544.
Winkler, L.W., 1888. Bestimmung des im Wasser gelösten Sauerstoffs. Ber. Dtsch. Chem. Ges. 21, 2843–2855.
Wooster, W.S., 1959. Oceanography observations in the Panama Bight, "Askoy" expedition, 194. Bull. Am. Mus. Nat. Hist. 118, 113–151.